Development of a Linear Compressor for Stirling-Type Cryocoolers Activated by Piezoelectric Elements in Resonance

S. Sobol, T. Sofer, G. Grossman

Technion – Israel Institute of Technology
Haifa, Israel 32000

ABSTRACT

A new drive mechanism for a linear compressor employing a piezo-actuator operating in resonance was developed theoretically and was built practically during this research. The compressor is designed to drive a miniature Pulse Tube cryocooler, particularly our MTSa model, which operates at 100 Hz and requires a filling pressure of 40 bar and a pressure ratio of 1.3. Since piezoelectric stack actuators generally possess a natural frequency on the order of 10 kHz, a resonance operation of the piezo compressor at 100 Hz was achieved by incorporating the piezo ceramics into the moving piston, and, additionally, by reduction of the effective piezo stiffness using hydraulic amplification.

An analytical spring-mass-damper model of the drive mechanism was developed and validated by the preliminary test setup, which showed a fine agreement between the simulations and the test results. According to the preliminary results and the simulations, the resonance operation of the piezo compressor improves the electromechanical efficiency by hundreds of percent relative to the quasi-static operation, in which the efficiency is on the order of merely ten percent. The high efficiency together with a no-moving-parts design can make a piezo compressor a good alternative to the conventional for applications requiring long life and reliability.

INTRODUCTION

Stirling cycle-based cryocoolers normally employ mechanical compressors activated by inductive electrical motors, which produce an oscillating pressure in the working gas. The main disadvantage of the conventional compressors is their limited lifetime which is caused by mechanical friction and wear. The wear products and outgassing of lubricants contaminate the working gas and thus degrade the cryocooler performances. Additional disadvantages are heat generation, induced vibrations and noise. In pulse tube cryocoolers, the pressure wave generator is a critical component, since it is the only mechanically active component subject to wear and failure. Therefore, the lifetime and reliability of the pulse tube cryocooler depends mostly on the compressor.

Conventional compressors are classified into rotary and linear motor types. A rotary compressor generally has a shorter lifetime than a linear one due to bearing wear and enhanced piston-cylinder wear caused by radial forces applied by the crank shaft mechanism.

Moreover, a rotary compressor produces a troublesome angular momentum, which is hard to eliminate or reduce. Disadvantages of the linear compressors are a lower efficiency, complicated electronic and control systems, increased weight and volume (particularly due to the electronics).

Cryocoolers 17, edited by S.D. Miller and R.G. Ross, Jr.

Gilbertson and Busch[1] first presented a survey of ten different methods of transforming energy into motion applicable to miniature actuators. According to the survey, the piezoelectric devices exhibit the highest efficiency, fastest speed of operation and highest power density relative to other methods. These advantages make the piezoelectric devices potentially attractive for implementation in miniature cryogenic compressors.

The major problem in employing the piezo actuators is an extremely small elongation of the piezo materials, which is about 0.1% of the total actuator length, and is on the order of microns in standard piezo actuators. Definitely such small strokes create technological problems in their implementation associated with the dimensional and geometry tolerances, surface finishing, structure stiffness and more. The second significant disadvantage of the PZT actuators is the undervalued power density and electromechanical efficiency at "low" operation frequencies. In fact, the direct quasi-static wave generation using piezo actuators at frequencies 50-150 Hz, suitable for a Stirling-type cryocooler, is extremely inefficient. In this case about 90% of the PZT charge is wasted, mostly due to the elasticity of the PZT ceramics itself. To improve the efficiency, it is essential to operate at the resonant frequency, which must fit the working frequency of the cryocooler.

Two fundamental approaches of the resonant operation, electrical and mechanical, are possible in our application, since both types may maximize the useful electromechanical efficiency of the PZT actuator. Operation at electrical resonance implies an installation of a particular RLC circuit, which should recover the electrical charge of the PZT, and thus minimize the power consumption. Operation at mechanical resonance, on the other hand, maximizes the mechanical output by means of recovering the potential mechanical energy stored in the system. Therefore, despite the equivalency of the methods in terms of the electromechanical efficiency, operation in mechanical resonance yields much higher power density, and is superior. However, forcing the PZT actuator to operate at resonance some orders of magnitude below its natural frequency is not a simple task. In case of a miniature pulse tube cryocooler the required frequency is about 100-150 Hz. Since the natural frequency of the PZT stack actuators is generally on the order of ten kHz, the compressor's mechanism must reduce the resonance frequency by 100 times.

As far as we know, there are various patents and publications regarding the employment of piezo actuators for gas compression or liquid pumping. Piezo compressors may be classified into two types: low frequency compressors operating in a quasi-static mode, and high frequency compressors, which employ a frequency reduction mechanism with complicated hydraulic transmission. The latter compressors are also unable to exploit piezo-operation at resonance because of the frequency limitations due to the check valves speed and increased hydraulic losses. Therefore, our concept of the direct gas compression with a piezoelectric actuator operating at low-frequency resonance is unique.

CONCEPT

The natural frequency of any mechanical system is proportional to the square root of the effective stiffness divided by the appropriate mass. In order to reduce the resonance frequency we propose to use a stroke amplification system for the PZT actuator, and, in parallel, to enlarge the mass of the compressing piston by adding the mass of the PZT ceramics itself and the PZT housing. Amplification of the PZT displacement reduces the effective stiffness of the PZT assembly by a factor equal to the square of the amplification ratio, and, therefore, is inversely proportional to the resonance frequency.

Figure 1 demonstrates the conceptual assembly of the linear compressor employing the new drive mechanism. The PZT stack actuator (red) is embedded into a stiff housing (green) with a rigid attachment on the right end of the stack. The left end of the PZT actuator is equipped with a moving piston of area A_1, which serves to compress the hydraulic liquid on its opposite side. The liquid space is bounded on the left side by a smaller piston, A_2, which is rigidly attached to the static envelope of the compressor (black). The Stirling-type refrigerator should be connected to the right end of the envelope, where the third piston, A_3, generates pressure oscillations in the embedded compression space. The third piston is rigidly attached to the right end of the PZT housing and, consequently, should possess the same displacement as the right end of the PZT actuator.

How does it work? The PZT actuator produces an internal force, F_e, at both ends in the axial direction, proportional to the applied voltage. As a result, the PZT ceramics tend to elongate, and the hydraulic volume on the A_1 side tends to decrease. In the absence of external load, reduction of the liquid volume on the A_1 side must be compensated by an increase in the length of the A_2 side by a factor A_1/A_2. Enlargement of the length on the A_2 side of the liquid volume is possible only by displacement of the PZT housing in the right direction, since the second piston, A_2, together with the envelope are assumed static. Thus, we obtain an amplified moving part of the compressor, which contains several masses, namely the PZT actuator, PZT housing, pistons A_1 and A_3, and some more. This moving part may be considered to be attached to the static envelope of the compressor by two supporting springs: gas spring of the load (cryocooler) and the stiffness measured at the A_2 piston. Ideally, the latter should be equal to the stiffness of the PZT stack divided by the square of the amplification ratio. Therefore, by choosing an appropriate ratio A_1/A_2 together with a relatively large moving mass it is possible to obtain a resonance operation of the PZT actuator assembly at frequencies considerably lower than the natural frequency of the PZT itself.

MODEL

Practically, the stiffness measured at the A_2 piston (Fig. 1) contains some additional in-series spring constants, such as stiffness of the amplification system, elasticity of the PZT housing and non-ideal mechanical contacts. These secondary springs may have a significant impact on the compressor dynamics, and thus, must be considered in the design. For a deeper understanding of the internal phenomena and for optimizing the compressor parameters, an analytical spring-mass-damper model was developed.

We split the continuous mechanism of the compressor by the section line shown on Fig. 1 into three moving parts, and thus, obtained a three-degrees-of-freedom model. According to the nomenclature of coordinates in Fig. 1, the right part of the PZT actuator combined with the right part of the PZT housing was denoted as the first model mass, namely m_1, the left part of the actuator together with the A_1 piston became m_2, and the left part of the PZT housing m_3. The third mass is connected with m_1 through the structural spring k_s, which defines the stiffness of the PZT housing. Damper c_3 is connected to m_3 in order to simulate the possible friction between the housing and piston A_2.

The hydraulic amplification system is assumed compressible, and is represented by a rigid mechanical lever with hydraulic spring k_h connected to the static envelope as shown on Fig. 2. The no-load amplification ratio is presented by means of the lever lengths, namely $a=l_1/l_2=A_1/A_2$

An intended cryocooler is supposed to apply a two component load on the compressor, namely a gas spring k_g and a damper c_1. Both components are attached to m1 in parallel. Physical interpretations of the gas and hydraulic springs are given by Eqs. (1) and (2) respectively:

$$k_g = \frac{\gamma P_{g0} A_3^2}{V_{g0}} \tag{1}$$

$$k_h = \frac{K A_2^2}{V_{h0}} \tag{2}$$

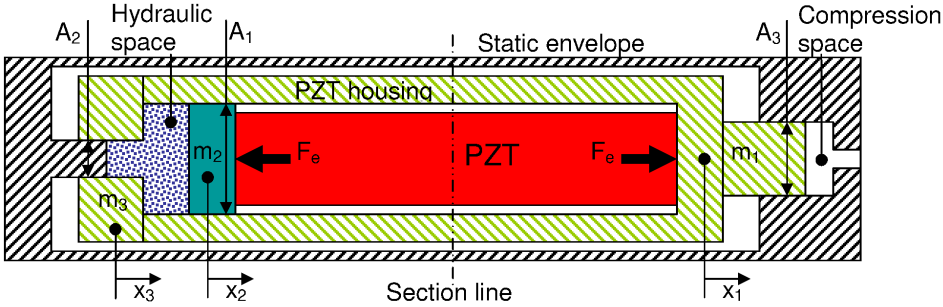

Figure 1: Schematics of the proposed linear compressor.

where γ, P_{g0} and V_{g0} are the adiabatic constant, the filling pressure and the mean volume of the cryocooler gas respectively; K and V_{h0} are the bulk modulus and the mean volume of the liquid. The amount of the liquid compression is expressed by vector x_4, shown on Fig. 2, according to Eq. (3):

$$x_4 = \frac{V_h - V_{h0}}{A_2} \tag{3}$$

In this paper the PZT model integrates both mechanical and electrical aspects of the PZT nature in order to estimate the current behavior in the vicinity of the resonance frequency. A piezo actuator, schematically bounded by a dashed line on Fig. 2, consists of masses m_1 and m_2 (partially) connected by the PZT stack stiffness k_P and the mechanical damper c_P. The force generator is embedded into an electrical circuit through the electromechanical converter with symmetric coefficient N. The converter is supplied with external voltage V in parallel with the PZT capacitor C_0[2,3]. The constitutive equations of the piezo stack in our application have the following form, omitting the irreversibility:

$$\begin{cases} A_1 P_h = k_P(x_1 - x_2) - NV \\ Q = N(x_1 - x_2) + C_0 V \end{cases} \tag{4}$$

where Q is the PZT charge, and the product NV, denoted in Fig. 2 by F_e, is the PZT force generated by the inverse piezoelectric effect. Differentiation with respect to time of the second equation in set (4) provides a differential equation for the PZT current:

$$I = N(\dot{x}_1 - \dot{x}_2) + C_0 \frac{dV}{dt} \tag{5}$$

Motion equations of the proposed model were obtained using the Euler-Lagrange method. Three independent vectors x_1, x_2 and α were chosen for the solution. Relations of x_3 and x_4 to the independent vectors are given in (6) (see Fig. 2 – Right). Angle α is assumed to be small enough to allow ignoring the vertical displacement of vectors x_3 and x_4.

$$\begin{cases} x_3 = x_2 + l_2 \sin\alpha \\ x_4 = x_2 - (a-1) l_2 \sin\alpha \end{cases} \tag{6}$$

The Lagrangian and the dissipation functions of the mechanical system are presented in Eqs. (7) and (8) respectively. Solution of the Euler-Lagrange equations is given in (9).

$$\begin{aligned} L = {} & \frac{1}{2} m_1 \dot{x}_1^2 + \frac{1}{2} m_2 \dot{x}_2^2 + \frac{1}{2} m_3 (\dot{x}_2 + l_2 \dot{\alpha} \cos\alpha)^2 - \\ & - \frac{1}{2} k_g x_1^2 - \frac{1}{2} k_P (x_1 - x_2)^2 - \frac{1}{2} k_s (x_1 - x_2 - l_2 \sin\alpha)^2 - \frac{1}{2} k_h (x_2 - (a-1) l_2 \sin\alpha)^2 \end{aligned} \tag{7}$$

$$D = \frac{1}{2} c_1 \dot{x}_1^2 + \frac{1}{2} c_P (\dot{x}_1 - \dot{x}_2)^2 + \frac{1}{2} c_3 (\dot{x}_2 + l_2 \dot{\alpha} \cos\alpha)^2 \tag{8}$$

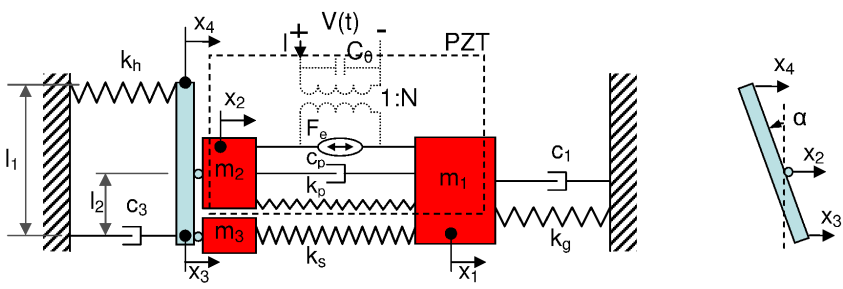

Figure 2: Left – Three mass model of the proposed linear compressor. Right –zooming on the mechanical lever in deflected mode.

$$\begin{cases} m_1\ddot{x}_1 + (c_1 + c_P)\dot{x}_1 - c_P\dot{x}_2 + (k_P + k_s + k_g)x_1 - (k_P + k_s)x_2 - k_s l_2 \sin\alpha = NV \\ (m_2 + m_3)\ddot{x}_2 + m_3 l_2 \ddot{\alpha}\cos\alpha - c_P\dot{x}_1 + (c_P + c_3)\dot{x}_2 + c_3 l_2 \dot{\alpha}\cos\alpha - m_3 l_2 \dot{\alpha}^2 \sin\alpha - \\ \qquad (k_P + k_s)x_1 + (k_P + k_s + k_h)x_2 + (k_s - (a-1)k_h)l_2 \sin\alpha = -NV \\ m_3\ddot{x}_2 \cos\alpha + m_3 l_2 \ddot{\alpha}\cos^2\alpha + c_3\dot{x}_2\cos\alpha + c_3 l_2 \dot{\alpha}\cos^2\alpha - m_3 l_2 \dot{\alpha}^2 \cos\alpha\sin\alpha - \\ \qquad k_s x_1 \cos\alpha + (k_s - (a-1)k_h)x_2\cos\alpha + (k_s + (a-1)^2 k_h)l_2 \cos\alpha\sin\alpha = 0 \end{cases} \tag{9}$$

The obtained motion equations can be linearized by assuming α close to zero. Thus, terms in (9) that include α^2 or its derivatives were omitted, sine and cosine of α were replaced by α and 1 respectively. As a result we obtained a linear set of the motion equations, which in matrix form is given in (10):

$$\begin{bmatrix} m_1 & 0 & 0 \\ 0 & m_2 + m_3 & m_3 \\ 0 & m_3 & m_3 \end{bmatrix} \begin{bmatrix} \ddot{x}_1 \\ \ddot{x}_2 \\ l_2\ddot{\alpha} \end{bmatrix} + \begin{bmatrix} c_1 + c_P & -c_P & 0 \\ -c_P & c_P + c_3 & c_3 \\ 0 & c_3 & c_3 \end{bmatrix} \begin{bmatrix} \dot{x}_1 \\ \dot{x}_2 \\ l_2\dot{\alpha} \end{bmatrix} + \begin{bmatrix} k_P + k_s + k_g & -(k_P + k_s) & -k_s \\ -(k_P + k_s) & k_P + k_s + k_h & k_s - (a-1)k_h \\ -k_s & k_s - (a-1)k_h & k_s + (a-1)^2 k_h \end{bmatrix} \begin{bmatrix} x_1 \\ x_2 \\ l_2\alpha \end{bmatrix} = \begin{bmatrix} NV \\ -NV \\ 0 \end{bmatrix} \tag{10}$$

Equations (10) and (5) together with relations (6), in which $\sin\alpha$ is replaced with merely α, are supposed to fully describe the dynamics of the proposed linear compressor model. Equation (10) is independent of (5) and (6), and thus, can be solved separately for any form of the supplied voltage V(t). Solutions for (5) and (6) can be obtained thereafter.

PROTOTYPE

A prototype of the innovative mechanism (Fig. 3) was developed theoretically and was built practically in order to validate the concept and the corresponding theoretical model. For simplicity

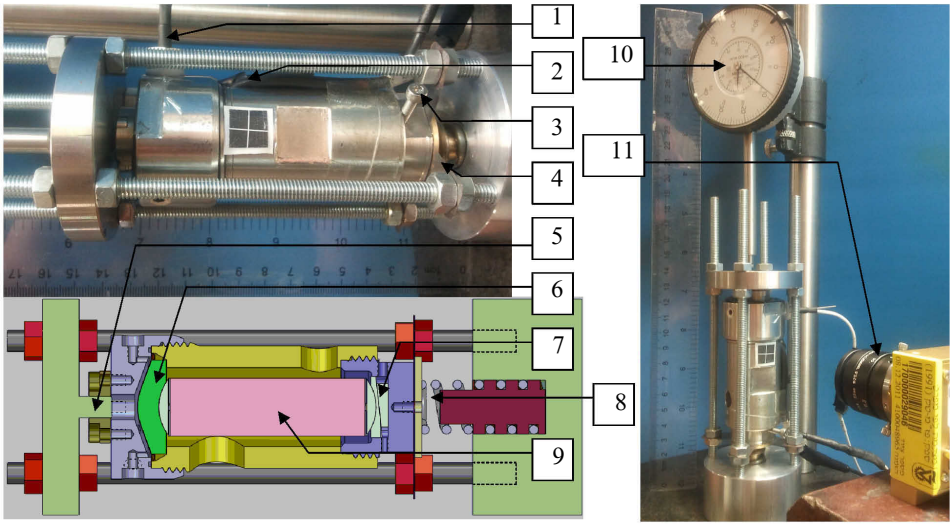

Figure 3: Prototype of the proposed drive mechanism with the test setup. (1) – Pressure gauge; (2) – Power supply and SGS wires; (3) – PZT placement fine tuning screw; (4) – Flexural bearing; (5) – Piston A_2; (6) – Piston A_1; (7) – PZT placement fine tuning mechanism; (8) – Load spring; (9) – PZT actuator; (10) – Analog micrometer; (11) – Fast video camera.

and wider measurement flexibility, the prototype was designed to operate at room atmosphere with a mechanical load (helical spring) instead of a gas spring. For the higher stiffness of the actuator-housing-amplifier assembly, some advanced design ideas were involved. Sockets for the spherical PZT caps were matched precisely by press finishing; large single threads were used for the housing assembly instead of the conventional flange connections; a metal flexure membrane of unique shape was involved in the primary piston (A_1).

The liquid volume was minimized in order to increase the hydraulic spring constant according to Eq. (2). Pure water was chosen for the amplifying system liquid, since it possesses relatively high bulk modulus and is bio- and chemically-friendly. The relatively high viscosity of the water has a minor effect on the system dynamics because of the insignificant strokes. Water sealing on the A_2 piston was performed by a neoprene sheet diaphragm. Certainly, this is not the ultimate method of sealing for long-term operation; however, the method is very easy for implementation and has a negligible influence on the mechanics.

The load spring is adjustable for the spring constant due to the ability of changing the effective length by screwing the reciprocal housing in and out. A flexural bearing was located between the helical spring and the PZT housing in order to eliminate possible tilt and torsion. The flexural bearing location is also adjustable according to the load spring tip location.

The compressor parameters were chosen to fit the requirements of our miniature MTSa pulse tube cryocooler[4], which operates at nearly 100 Hz, requires a filling pressure of 40 bar and a pressure ratio of 1.3. The effective mean volume of the cryocooler is about 0.7 cc. Assuming a 12mm diameter compression piston with 1 mm stroke the mean compression volume increases up to 0.76 cc, and according to Eq. (1), the gas spring constant becomes equal to 113 N/mm in this case. The actual helical spring in the experiment setup together with the flexural bearing can provide the spring constant up to 120 N/mm.

In recent work, we employed a high voltage stack PZT actuator P-016.40 of PI® with 60μm elongation, 100 N/μm stiffness, and 680 nF capacity. Spherical caps were glued upon the PZT tips in order to allow symmetric self adjustment of the actuator in the negative spherical sockets, and thus-to prevent bending forces. A fine tuning mechanism for the PZT placement was embedded into the PZT housing in order to control the A_1 and A_2 piston locations. The tuning can be performed by two external screws at any time of operation.

Selection of the A_1 piston diameter was restricted by the PZT parameters and the hydraulic pressure, since the dynamic operation of the PZT stack actuator must be accompanied by application of a specific pre-load on the piezo stack. According to recommendations of the PZT manufacturer[5], the mean pre-load should result in half the maximum allowable PZT shrinkage, which is about 30μm in our case. Therefore, assuming the mean hydraulic pressure of 50 bar, the A_1 piston diameter was set at 28 mm.

In contrast with A_1, selection of the A_2 piston diameter was more arbitrary, and depended mostly on the required amplification ratio, which in turn strongly affected the resonance frequency. Unfortunately, according to Eq. (2), A_2 strongly affects the hydraulic spring constant also. Therefore, establishing a larger amplification ratio implies the softening of the hydraulic spring, and in case of a springy load, results in a less effective amplification system. According to preliminary simulations employing the theoretical model, the A_2 piston diameter was set at 6.5 mm as a compromise.

EXPERIMENTAL SETUP

Our experimental setup allows five types of real time data measurements on the PZT compressor mechanism: PZT elongation is measured by a full bridge SGS mounted on the piezo ceramics, hydraulic pressure by the installed pressure gauge, PZT housing displacement by a fast video camera, PZT current and PZT voltage by the circuit embedded into the power supply (see Fig. 3). The camera is calibrated by an analog micrometer at low frequencies. The signal to the PZT actuator and the measured data are controlled by DasyLab™ software.

In order to validate the theory, some model values were complemented by specific tests and measurements on the actual prototype mechanism. For example, a special test was performed in

order to estimate the constant k_s. By means of a controlled syringe-like device connected to the hydraulic amplifier, a pressure-to-volume relation curve was obtained. Based on the known spring constants and the obtained curve, k_s was estimated as a function of the pressure. It was found that k_s has a constant value of 480 N/µm at pressures higher than 20 bar. At lower pressures the structure stiffness degrades drastically down to about 50 N/µm at the atmospheric pressure in the hydraulic amplifier.

Prior to the high frequency response experiments, the prototype was tuned for the ultimate quasi-static operation. Once the amplification system volume was filled completely with water (no gas bubbles), the prototype was placed in the test casing, covered by the A_2 piston flange, and tightened with four nuts gradually for obtaining perfect piston-cylinder coaxiality and, additionally, for obtaining a sufficient pre-load on the load spring and on the PZT actuator through the increased pressure in the amplifier. The initial pressure was set to 40 bar, which resulted in 2.5 kN pre-load on the PZT stack and in 25 µm of the initial PZT shrinkage. The nuts tightening procedure was accompanied by running the PZT actuator at 1 Hz and by real time observation of the measured data. Measurement of the PZT housing stroke by an analog micrometer indicated the quality of assembly: the ultimate orientation of the tightened flange provided the maximum stroke and, in addition, the minimum pressure amplitude. As a final step the flexural bearing nuts were tightened for maintaining the bearing springs around the flat equilibrium.

RESULTS AND DISCUSSION

Figure 4 illustrates a summary of both experimental and theoretical frequency responses of the compressor mechanism for a 200 V peak to peak sine driving voltage in the range of frequencies up

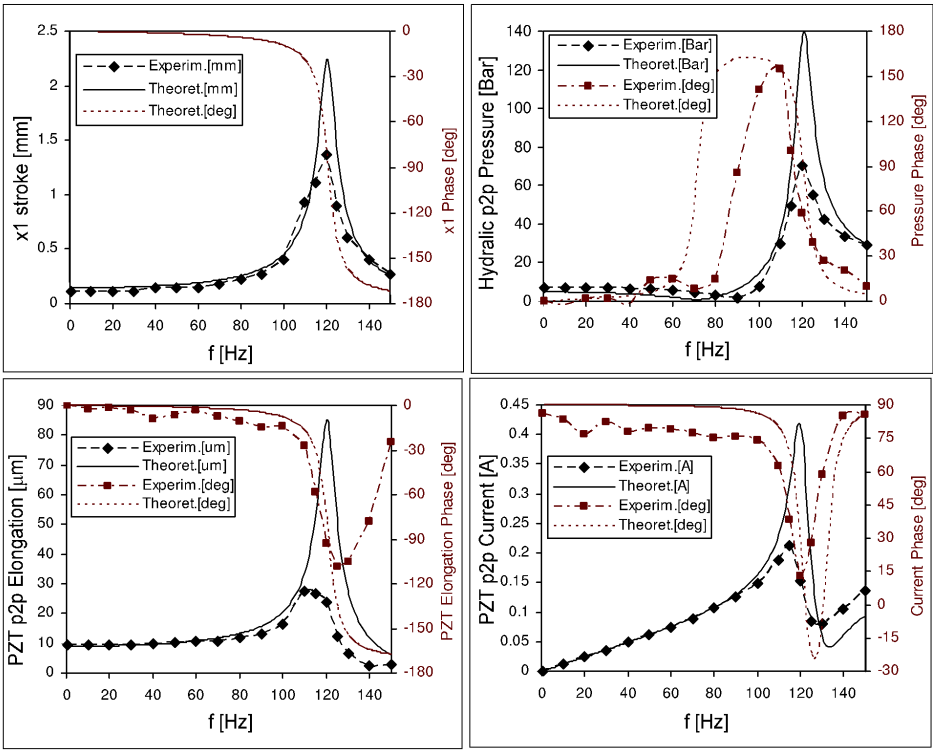

Figure 4: Frequency response of the prototype and the corresponding theoretical model.

to 150 Hz. Numerical values used in the simulations are the following: a=18.56, m_1=0.25 kg, m_2=0.05 kg, m_3=0.25 kg, k_s=480 N/µm, k_P=100 N/µm, k_h=1222 N/mm, k_g=113 N/mm, c_1=20 Ns/m, c_3=5 Ns/m, c_P=1000 Ns/m, C_0=680 nF, N=6 N/V. The left ordinates show the peak to peak amplitudes of the measured parameters, while the right ordinates show their phases relative to the voltage sampled on the power supply. Additionally, during the actual operation at above 120 Hz, the voltage amplitude started to decrease because of the power supply limitations, and therefore, the measured voltage divided by the nominal 200 V was used as a correction factor for the other measured amplitudes.

In accordance with the concept and the corresponding theoretical model, the PZT mechanism together with the PZT actuator entered the resonance mode at relatively low frequency, suitable for operation of a miniature pulse tube cryocooler. The ultimate operation frequency of the prototype obtained was 120 Hz, which provided both maximum amplitude of the load spring (simulating the gas spring) and minimum current phase.

Relative to the quasi-static mode, the x_1 stroke obtained was amplified 11.4 times in resonance, namely from 0.12 mm to 1.37 mm, and the PZT elongation amplitude increased 2.9 times, namely from 9.4 to 27.4 micrometers. Since the PZT housing stroke was measured separate from the other parameters (by video), the x_1 experimental phase does not appear on the x_1 plot of Fig. 4. Nevertheless, according to the good agreement between the experimental and theoretical amplitude curves, one can assume the actual phase behavior to be quite close to the theoretical.

According to the theoretical and experimental curves of the liquid pressure, one can see the antiresonance appearing at 90 Hz and 71 Hz respectively. The lowest amplitude of the pressure is accompanied by a 90 degrees phase of the pressure in both cases. Despite some disagreement in the antiresonance frequencies, the first resonance frequency of the amplified liquid pressure, as well as that of the PZT housing, was obtained as predicted at 120 Hz. At this frequency point the pressure phase crosses the 90 degrees line for the second time, and drops to zero thereafter.

The results show that at low frequencies the actual x_1 stroke is 20% lower than the predicted one, while the pressure oscillation in the hydraulic liquid is about 50% higher. This fact indicates that the moving system was mechanically restrained to some extent, most likely by the dry friction on the A_2 piston. On the other hand, in the vicinity of the resonance frequency the pressure amplitude obtained was about twice lower than predicted by the model, and unfortunately, it resulted in much reduced amplitude of the actual PZT elongation relative to the theoretical one, and consequently, in the limited current amplification.

Moreover, the maximum PZT elongation was obtained slightly before the expected, namely between 110 and 115 Hz, although the PZT phase dropped to -90 degrees at exactly 120 Hz, which fits the main resonance frequency. The expected antiresonance of the PZT elongation was obtained before the predicted frequency, namely at 140 Hz instead of 190 Hz. Both experimental and theoretical antiresonances were accompanied by -90 degrees of the PZT phase. Similar to the experimental curve, the theoretical PZT elongation phase returns to zero slightly after the antiresonance, namely at about 210 Hz (see Fig. 5).

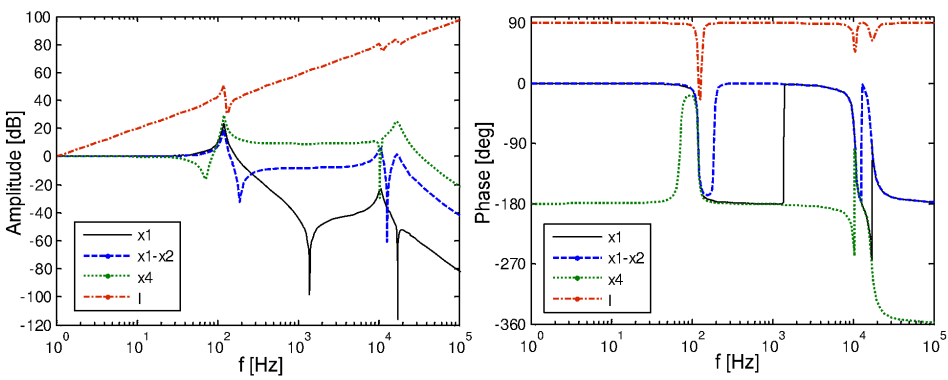

Figure 5: Extended frequency response of the theoretical model.

Corresponding to the PZT amplitude, the current peak to peak amplitude reached the maximum of 213 mA at 115 Hz, while the minimum current phase was obtained at 120 Hz, where the current amplitude dropped by 30% relative to the current peak. Note that according to the model the current was expected to reach the maximum amplitude at 120 Hz and the minimum phase at 125 Hz. In the quasi-static range of frequencies, up to around 80 Hz, a fine agreement is obtained between the experimental and theoretical curves of both PZT elongation and current.

In our application the current-to-voltage phase is the most important parameter with regard to the electromechanical efficiency. Since our power supply does not possess a charge recovery system, the reactive electrical power is merely wasted. Zero phase of current implies vanishing of the reactive power, and thus, results in complete consumption of the supplied electric power by means of the real power, which, omitting the losses, is intended to be converted into the PV power for the cryocooler.

According to the experimental results, at 120 Hz the current amplitude was 76 mA with 13 degrees of phase relative to the 100 V amplitude voltage. Therefore, the mean apparent electrical power was 3.8 VA, while the real power consumption was obtained at 3.7 W by multiplying the apparent power by the cosine of 13 degrees, which is 0.974. The mechanical output at 120 Hz was estimated using the c_1 and c_3 parameters from the theoretical model, which in total gave 25 Ns/m of the damping constant applied to the PZT housing. Therefore, the real part of the mechanical power was estimated at 3.3W and the total electromechanical efficiency of the system at 87% based on the apparent electrical power. To compare, at 100 Hz the corresponding efficiency is merely 5.3% because of the reduced mechanical amplitude and close to 90° phase of the PZT current, though the current amplitude is similar to the one obtained at 120 Hz. Based on the real electrical power the electromechanical efficiency at resonance was close to 90%, which indicates that about 10% of the electrical power was consumed in terms of heat due to mechanical, dielectric and resistive losses of the PZT material.

Due to the satisfactory agreement obtained between the theoretical and experimental results at the tested frequencies and due to a limited ability to provide experiments at the higher frequencies, the extended frequency response, shown in Fig. 5, presents only the theoretical results. According to the model prediction, the second system resonance occurs at 10,610 Hz, which is two orders of magnitude larger than the operational resonance frequency. Such large difference between the frequencies implies an ignorable influence of the higher motion modes on the low frequency operation. Therefore, the system may be simplified down to one-or two-degree-of-freedom model by combining the three mass values into m1 or into m_1 and m_2 respectively and canceling other masses in Eq. (10) thereafter. An appropriate simulation showed that up to about 1000 Hz both two-and three-degrees-of-freedom models demonstrate identical results.

SUMMARY AND CONCLUSIONS

A new concept of the drive mechanism for a Stirling-type-cryocooler compressor employing a piezo actuator operating in resonance was developed theoretically and validated practically during the research. The prototype demonstrated a stable operation at 120 Hz providing a 1.37 mm stroke of the dedicated 12 mm diameter compression piston with a damping coefficient estimated at 25 Ns/m, while the PZT actuator was supplied by 1/5 the maximum voltage amplitude. At the resonance frequency the actuator demonstrated a peak to peak elongation of 24 microns, while the maximum allowable is 60 µm. Therefore, assuming linear scaling, the maximum piston stroke for the given conditions can be estimated at 3.43 mm for 500 V peak to peak voltage supply, while the higher voltage is limited by the PZT elongation. The resulted amplitude is quite sufficient to fulfill the requirements of our MTSa pulse tube cryocooler[4].

A current-to-voltage phase shift was achieved from almost 90 degrees for quasi-static operation down to 13 degrees in resonance. Since the cosine of the obtained phase is close to one, the electromechanical conversion based on the apparent electrical power was almost at maximum and was estimated at 87% for the given PZT actuator.

The analytical linear spring-mass-damper model of the drive mechanism was validated by the experimental setup, and showed a perfect qualitative and a fine numerical agreement with the ob-

tained results. The model predicted correctly the main resonance frequency and, qualitatively, all the system operating parameters, despite some inaccuracy in their values, especially in the amplitudes.

In the resonance vicinity the main reason for the decreased amplitudes of the prototype relative to the theoretical appears to be the nonlinear behavior of the structural stiffness, which drops strongly at low hydraulic pressures. Since the pressure varies with high amplitude in this region, the actuator-to-housing coupling loses its intensity as the pressure drops, and the PZT does not receive a sufficient impact by the system. To avoid this problem one can raise the initial amplifier pressure; however, this approach requires some changes in the system design. The second reason for the discrepancies between the model and the prototype is the linear approximation of the actual parameters.

Conclusively, the research demonstrated an ability of effective employment of a piezo actuator in a Stirling-type-cryocooler compressor. The corresponding model was validated and can be used for optimization of the actual compressor parameters. A no-moving-parts design of the proposed compressor is applicable due to relatively low amplitudes, which allow replacement of the piston-cylinder assemblies by flexural bearings and membrane seals. Additionally, an in-line configuration of the compressor consisting of two opposite PZT based compression units of smaller size should reduce the amplitudes even more, and, additionally should eliminate the enhanced vibrations. The high efficiency together with a no-moving-parts design can make the double piston piezo compressor a good alternative to the conventional, for applications requiring long life, reliability and silent operation.

ACKNOWLEDGMENT

The generous financial help of the Rechler Family, MAFAT and the Technion is gratefully acknowledged.

REFERENCES

1 Gilbertson, R.G. and Busch, J.D., "A Survey of Micro-Actuator Technologies for Future Spacecraft Missions," *Journal of The British Interplanetary Society*, Vol. 49 (1996), pp. 129-138.

2 Setter, N., "ABC of Piezoelectricity And Piezoelectric Materials," Proceeding of the International Conference on Piezoelectric Materials for End Users, (2002), INTERLAKEN, Switzerland.

3 Wang, S.H., Tsai, M.C., "Dynamic modeling of thickness-mode piezoelectric transducer using the block diagram approach," *Ultrasonics*, Vol. 51, Issue 5 (July 2011), pp. 617–624.

4 S. Sobol, Y. Katz and G. Grossman (2010): "A Sudy of a Miniature In-line Pulse Tube Cryocooler," *Cryocoolers 16*, ICC Press, Boulder, CO (2011), pp. 87-95.

5 Physik Instrumente (PI) Tutorial: "Piezoelectrics in Positioning," http://www.piceramic.de/, http://www.physikinstrumente.com.